Journal of Manufacturing Processes 28 (2017) 336–342

Contents lists available at ScienceDirect

Journal of Manufacturing Processes

journal homepage: www.elsevier.com/locate/manpro

Temperature field and microstructure characterization of AA6061/H70 dissimilar thermo-compensated resistance spot welds having different joint configurations

Yu Zhang[a,b], He Shan[a,b], Zhen Luo[a,b], Yang Li[a,b,*], Jing Bi[a,b], Jing Guo[a,b], Feng Gao[c]

[a] School of Materials Science and Engineering, Tianjin University, Tianjin 300350, China
[b] Tianjin Key Laboratory of Advanced Joining Technology, Tianjin University, Tianjin 300350, China
[c] Ansteel Mining Engineering Corporation, Anshan 114001, China

ARTICLE INFO

Article history:
Received 13 April 2017
Received in revised form 9 June 2017
Accepted 24 June 2017

Keywords:
Resistance spot welding
Dissimilar metal joining
Thermo-compensated method
Finite element modeling

ABSTRACT

Two types of dissimilar AA6061/H70 thermo-compensated resistance-spot-welding joint configuration are designed. Thermal-electric coupled finite element models are built to reveal the temperature field of these two types of joint. An AISI 201 stainless-steel thermo-compensated sheet assists resistance spot welding through heat conduction. The nugget formation is mainly due to conductive heat from this cover sheet when the thermo-compensated sheet is set adjacent to the AA6061 workpiece (type A joint) and is driven by both Joule heat and conducted heat when the cover sheet is set adjacent to the H70 workpiece (type B joint). To ensure the nugget formation, the conducted heat portion requires a long welding time while the Joule heat portion requires a high welding current. The type B joint configuration has higher Cu and Zn contents in the fusion zone, which leads to a high intermetallic content in the Al-Cu-Zn ternary system existing in the nugget. Most type A joints thus have a higher peak load than type B joints in tensile shear tests.

1. Introduction

Resistance spot welding (RSW) is a major method of assembling thin metal sheets that has the benefits of high productivity and high joining quality [1–3]. Some nonferrous metals (i.e., aluminum, magnesium, and brass) pose challenges in RSW because of their physical properties, such as their high thermal and electrical conductivity. Based on the typical RSW process, numerous derivative joining methods have been developed in recent decades to meet different demands. For instance, weld-bonding technology has been used to improve the static and dynamic mechanical properties of spot welding joints [4]. Additionally, a novel process called resistance element welding (REW) was introduced by the automotive industry to improve the joining quality of dissimilar Al/steel materials (which was a pressing demand for reducing vehicle mass) [5].

It has been widely demonstrated that the novel process mentioned above has advantages in terms of the mechanical performance of the spot welding joints of similar and dissimilar metals [6]. Despite the obvious merit of the new method, traditional RSW is still a vital joining process for thin-walled metal structures [7]. The priorities of a spot joining technique are the operating speed and robustness of the process. The weld-bonding process requires a solidification period at room temperature or ~150 °C afterward, which prolongs the production cycle. Additionally, the use of epoxy-based adhesives leads to a narrow welding lobe owing to the tendency of expulsion [8]. A sound Al/steel joint with strong ability to bear tensile shear loads can be realized by REW [5]. However, an additional hole-punching step makes the REW a two-step process, which limits the application of REW in the automotive industry. There is a need to develop a spot joining technique that is easily applied and produces highly robust joints.

Zhou et al. studied the weldability of thin nonferrous sheet metals (i.e., aluminum, brass, and copper) in small-scale RSW [9]. The weldability decreases in the order of aluminum, brass, and copper owing to the integrated effects of electrical resistivity, thermal conductivity, and the melting point. However, it is impossible to weld a pure-copper workpiece in regular or large-scale RSW. Recently, RSW with a thermo-compensated auxiliary has been developed to solve the problem of low heat generation for nonferrous metal during the joining process. Cover plates or processing tapes are set

* Corresponding author at: School of Materials Science and Engineering, Tianjin University, Tianjin 300350, China.
E-mail address: liytju@163.com (Y. Li).

http://dx.doi.org/10.1016/j.jmapro.2017.06.014
1526-6125/

Table 1
Chemical composition of AA6061 (wt-%).

Cu	Mg	Si	Mn	Zn	Cr	Ti	Fe	Al
0.15–0.4	0.8–1.2	0.4–0.8	≤0.15	≤0.25	0.04–0.35	≤0.15	≤0.7	Bal.

Table 2
Chemical composition of H70 (wt-%).

Cu	Zn	Pb	P	Fe	Sb	Bi	Other
68.5–71.5	Bal.	≤0.03	≤0.01	≤0.1	≤0.005	≤0.005	≤0.3

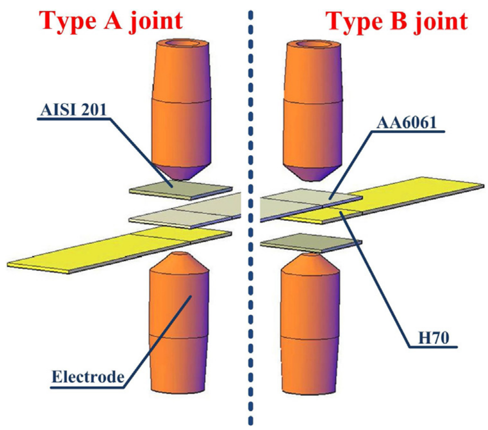

Fig. 1. Schematic of two joint configurations.

on one or two of the electrodes to improve the welding quality without introducing an additional processing step. Qiu conducted a parametric study of RSW with a cover plate for the magnesium alloy AZ31B [10]. Zhao successfully joined ultra-thin automotive sheets by inserting metal strips between parts and electrodes [11]. Dissimilar Al/Cu spot joining has been achieved employing a thermo-compensated method [12]. However, no study has focused on joining dissimilar Al/brass by thermo-compensated RSW, the metallurgical process of which is more complex than that of Al/Cu spot joining (because brass introduces Zn into the conjunct fusion zone). There is a shortage of Cu output worldwide, and it is thus necessary to investigate such a promising dissimilar nonferrous metal joining method to advance future application to Al/brass hybrid structures.

The present work investigated the effect of the joint configuration on the temperature field distribution across the cross-sections of Al/brass thermo-compensated resistance spot welds employing the finite element method (FEM). Two types of microstructure in the fusion zone were revealed for two types of joint.

2. Materials and experimental procedure

A 1-mm-thick sheet of aluminum alloy 6061 (AA6061) and single-phase brass H70 were selected in this work; chemical compositions are given in Tables 1 and 2 respectively. Prior research has shown that it is practical to use a 1-mm-thick AISI 201 stainless-steel sheet as an additional heat-generating material (i.e., cover sheet). Owing to the large difference in the thermal expansion efficient between 201 stainless steel and the workpiece [10,12], this cover sheet would separate from the welds during a cooling period. A pair of RWMA class-II C18200 electrodes with 6-mm tip ends were used.

A 220-kVA pneumatic-inverter RSW machine was used in this study. A schematic of Al/brass thermo-compensated RSW is shown in Fig. 1. To explore the welding lobe, for each joint configuration type, the welding current was varied from 6 to 12 kA in intervals

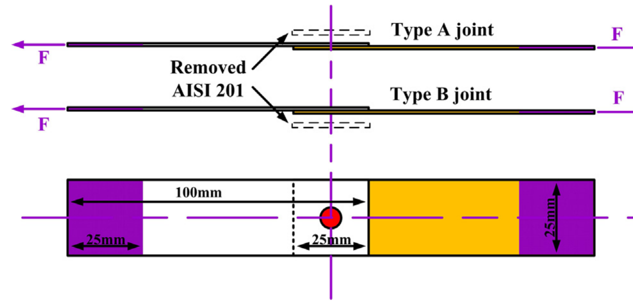

Fig. 2. Dimensions of a sample in the tensile shear test.

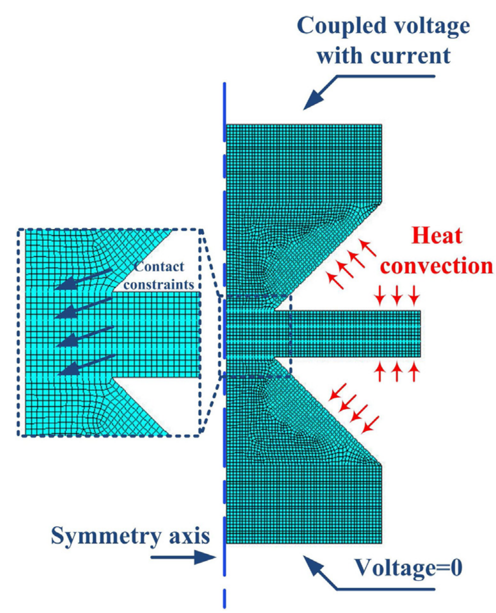

Fig. 3. Boundary conditions for the modeling of AA6061/H70 dissimilar thermo-compensated RSW.

of 1 kA; the welding time was incrementally increased as 100, 300, and 500 ms; and the electrode force was fixed at 3.6 kN.

The microscale structures of Al/brass dissimilar welds were observed along cross-sections after welding with an Olympus GX51 metallographic microscope and an FEI Inspect^{TM} S50 scanning electron microscope (SEM) equipped with an energy dispersive spectrometer (EDS). All samples were etched using Keller's reagent (i.e., 2.5 ml nitric acid, 1.5 ml chlorhydric acid, and 95 ml H_2O).

Samples (having the dimensions shown in Fig. 2) were put on a CSS-44100 material test system under a tensile speed of 1.0 mm min^{-1} to measure their abilities to bear a tensile shear load. Average results were recorded for three samples having the same welding parameters. The dimensions of a sample in the tensile shear test are shown in Fig. 2. Diameters of nuggets were recorded after the tensile shear test and the fracture surface of the joints examined using the SEM.

3. Finite element modeling

A simplified two-dimensional axisymmetric finite element model is established using FEM code ANSYS as shown in Fig. 3. In the model, a symmetry boundary condition is set along the central axis and thermal-electrical coupled PLANE 67 elements are used to show the difference in the temperature field distribution under different joint configurations. The model was composed of 11125 elements and 11790 nodes. The electrical potential at the bottom of the lower electrode is fixed to zero while the electrical